Nucleation and growth during a fluorogenic precipitation in a micro flow mapped by fluorescence lifetime microscopy

Vu-Long Tran, Valérie Génot, Jean-Frédéric Audibert, Robert B. Pansu*

Yury Prokazov,[±] Evgeniy Turbin,[±] Werner Zuschratter,[±]

Hyeong-Ju Kim,[°] Jaehun Jung,[°] Soo Young Park[°].

Laboratoire PPSM ENS Cachan, CNRS, UMR n 18531 & IFR d'Alembert IFR121
61, avenue du Président Wilson, 94235 Cachan cedex, France.
*Corresponding author, e-mail: robert.pansu@ppsm.ens-cachan.fr
Fax: +33 (0)1 47 40 24 54
Tel: +33 (0)1 47 40 53 38

[±] Leibniz Institute of Neurobiology, Magdeburg, Germany

°Center for Supramolecular Optoelectronic Material
32dong 409ho, Seoul National University, #599, Gwanak-ro, Gwanak-gu 155-744 Seoul, South Korea

S1. Laser and microscopy setup

Laser source

T- Pulse 200 (Amplitude system, Bordeaux, France): Gain media Yb:KYW crystal; average power 2.5 W; repetition rate 10 MHz; pulse width 400 fs; beam size around 1.27 mm. The laser is self-mode-locked by a Semiconductor Saturable Absorber Mirrors (SESAM) system. The original wavelength is 1030 nm.

Nonlinear optical crystal

The 2 nonlinear optical crystals were made from Beta Barium Borate (BBO) and were used to generate a second harmonic visible beam (515 nm) and a third harmonic UV beam (343 nm).

Mirrors and lenses

Certain mirrors and lenses were selected and properly aligned in order to adjust the beam direction and size.

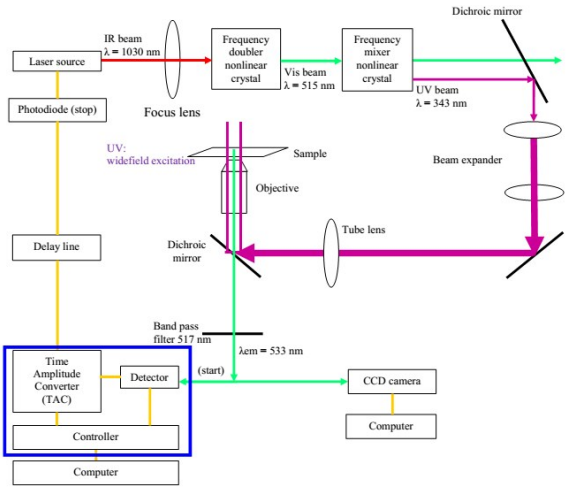

Fig S1. Laser and microscopy setup

Microscope

Inverted microscope Eclipse TE 2000-U (NIKON, Japan) was used with a dichroic mirror below the objective for the laser excitation at 343nm. Two ports were opened and closed to direct the emitted fluorescence to either a CCD camera or a single photon counting detector. Objectives with x20 (NA=0.45) magnification and microscope magnification module x1.5 were used to observe samples.

Bandpass

Due to the strong ability of UV light to excite unwanted materials in the environment, a BrightLine® single-band bandpass filter 517 ± 10 nm (Semrock, USA) was put above the exit to make sure only fluorescence coming from DBDCS was collected.

CCD camera

High and fast resolution Coolsnap HQ2 (Photometrics, USA) with 1392 x 1040 imaging pixels (6.45 x 6.45 µm) was used later and allow taking images with longer exposure times. Images were sent to a computer and processed in situ by Winview/32 (v. 2.5) (Princeton Instruments, USA).

Single photon counting detector

Widefield Time and Space correlated single photon counting (TSCSPC)-System with Large-Area-Detectors (Leibniz Institute for Neurobiology at Magdeburg, Germany) with a spatial resolution 40 µm on a cathode of ϕ=25mm and a time resolution of 60 ps was used to collect the fluorescent intensity and the lifetime from every pixel of the image. Data were sent to a computer and processed in real time by the LnTCapture software, and analyzed later with a home-made macro run in IGOR Pro (v. 6.3) (WaveMetrics Inc., USA).

The laser and the whole microscopy setup were aligned as shown in Fig S1. Finally, on the sample, we are able to excite by UV light (343 nm) in a widefield configuration.

S2. Physical, photophysical and morphological properties of DBDCS

Solubility is determined by measuring absorption at 380 nm of diluted samples in THF of saturated solutions at different ratios of THF and water, the fitted curve was established using the Jouyban – Acree model for predicting the solubility of organic molecules in aqueous binary mixtures[1].

$$\log S_{mix} = f \log S_T + (1-f)\log S_w + JA$$

$$f = \frac{V_{THF}}{V_{THF} + V_{H_2O}}$$

$$JA = f(1-f)\left[\frac{724.21}{T} + \frac{485.17(2f-1)}{T} + \frac{194.41(2f-1)^2}{T}\right]$$

T: room temperature (23^{0}C, 296 K)

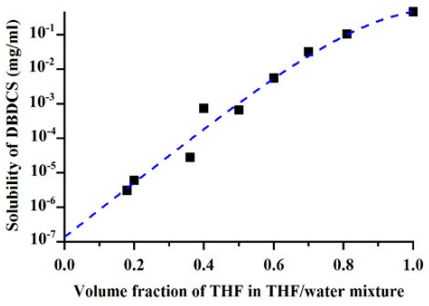

Fig S2a. Experimental solubilities of DBDCS in different mixtures of THF and water

Where S_{mix}, S_T, S_W are the solubility (mg/ml) of DBDCS in THF/water mixture, pure THF and pure water respectively; f is the volume fraction of THF and JA is the Jouyban-Acree factor which is based on the value calculated for ethanol – water mixtures.

Table S2b.

DBDCS	In THF solution	In THF/water (4:1) (NPs)	Solid state
Absorption peak	380 nm	349 nm	349 nm
Emission peak	Almost no emission	533 nm (green phase)	533 nm (G-phase) 458 nm (B-phase)
Quantum yield (Φ)	0.0026	0.62	N/A
Lifetime (τ)	4.2 ps	11.9 ns	23.9 ns (G-phase) 6.1 ns (B-phase)
Crystal morphology	-	-	Yellow (G-phase) Green (B-phase)

The solvatochromisme of DBDCS has been described in the Supplementary Information of ref 13. This file as well as the crystallographic information files are available at : http://pubs.acs.org/doi/suppl/10.1021/ja1044665

S3. Fluorescence decays of DBDCS solutions in THF at different concentrations

The fluorescence decays of DBDCS solutions in THF with increasing concentrations (from 0.1mg/mL to 0.5mg/mL) were measured. A component with a higher lifetime than that of the monomer (60 ps, instrumental response) was observed that can be attributed to dimers and/or higher oligomers.

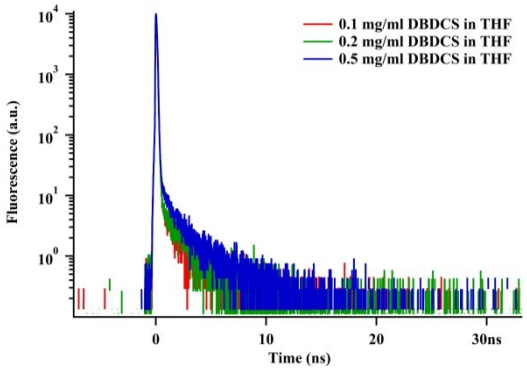

Fig S3. Fluorescence decay of DBDCS solutions in THF

S4. FLIM image time and space analysis by Principal Component Analysis algorithm

For each pixel, for each time t during the acquisition, we have stored the number of photons I collected for a given fluorescence delay τ: $I(X,Y,\tau,t)$. From that, we can calculate the fluorescence decay associated with a given Region Of Interest (ROI) and a given period of integration Δt.

$$I_{ROI}(\tau) = \int_{ROI}\int_{\Delta t} I(X,Y,\tau,t)\,dX\,dY\,dt$$

We assume to collect m ROIs in total from different regions.

Decays can be described as vectors with 4096 coordinates. If we define a scalar product in this space as:

$$I_\alpha(\tau).I_\beta(\tau) = \sum_{k}^{Channels} I_\alpha(k)\,I_\alpha(k)$$

The norm squared $I_\alpha(\tau).I_\alpha(\tau)$ is interpreted as a variance and is said to evaluate the amount of information that is provided by the data[2].

Description of the data

The PCA allows us to build an orthonormal base so that:

$$I_{ROI\ i \in [0,m-1]}(\tau) = \sum_j a_{ij} CP_j(\tau)$$

where the components $CP_i(\tau)$ are orthogonal one with respect to the others and have a norm of 1. The previous relation can also be written using matrix as:

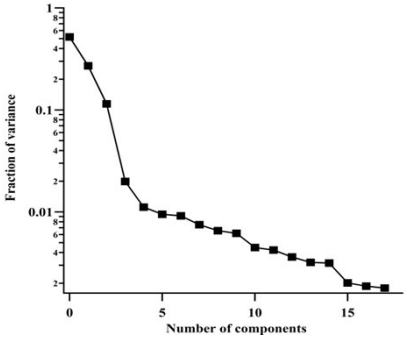

Fig S4a. Fraction of variance calculated by PCA

$$\underset{[I_{ROI}]}{\overset{m}{\frown}} = \underset{[CP_j]}{\overset{m}{\frown}} [a_{ij}]\}m$$

The CP(τ) have the same nature and units as decay, but they can have negative or non-integer counts in their channels.

One can check that $\sum_i a_{ij}^2$ is the contribution of the component $CP_j(\tau)$ to the description (variance) of the total data. We can sort the components CP based on their contribution.

Reduction of the number of component or species.

By reducing the description of the data to the 'imp' most important CP, we lose in the quality of the description but we gain in simplicity.

$$\underset{[I_{ROI}]}{\overset{m}{\frown}} = \underset{[CP_j]}{\overset{imp}{\frown}} \underset{[a_{ij}]\}}{\overset{m}{\frown}} imp + [R]$$

[R] is the matrix of the residuals.

$[\frac{R}{\sqrt{I_{ROI}}}]$ is the weighted residual matrix. It is displayed on figure S4b.

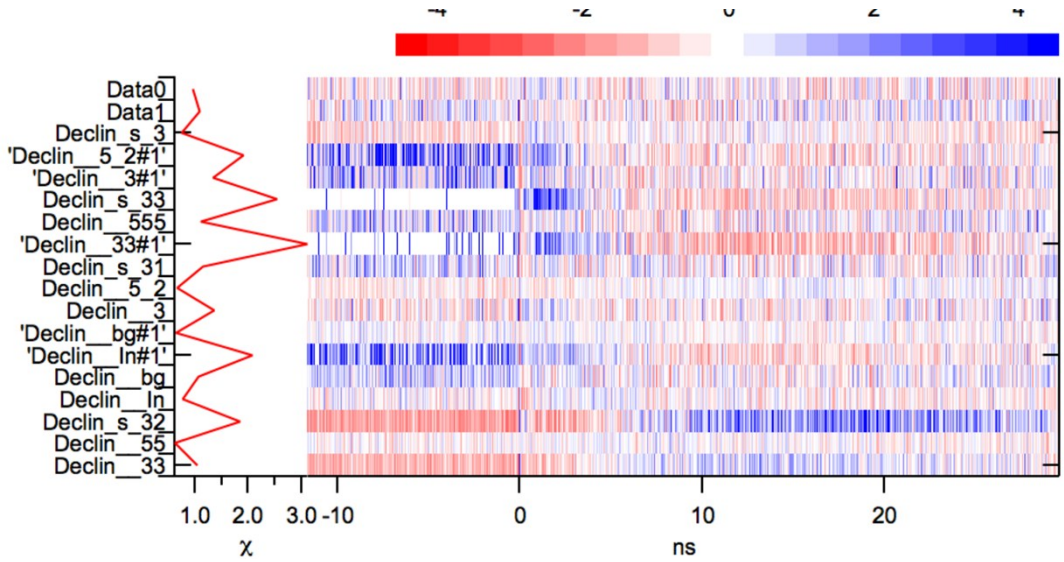

Fig S4b. The weighted residual matrix is displayed. It is the difference between the data and their description by the three first components. The weighted residuals fluctuates between ± 4. For each decay the variance X^2 of the distribution of the weighted residual is calculated. It should be close to one. The sign of the residual should change randomly. Domains where one colour dominates are domains where the data are not well described.

If it is possible to define 'imp' reference decays of known species, they can be approximated on the same base.

$$\underset{[Ref]}{\overset{imp}{\frown}} = \underset{[CP_j][b_{ij}]\}}{\overset{imp}{\frown}}\ \overset{m}{\frown}\ imp + [R_{ref}]$$

$[R_{ref}]$ is the matrix of the residuals. B=$[b_{ij}]$ is the decomposition of the decays of the known species on the orthogonal base.

$[\frac{R_{ref}}{\overline{Ref}}]$ is the weighted residual matrix.

This is the second point where model will defer for data.

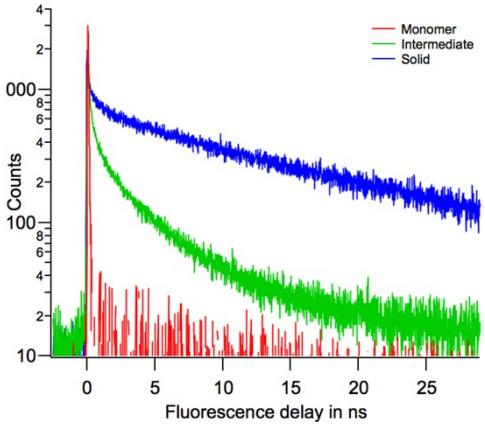

Fig S4c. Fluorescence decays of the three known species.

Construction of the decay of the reference species.

The monomer and solid decays can be obtained easily from the decays of the first and last images. The decay of the intermediate specie was constructed. It was constructed as a linear combination of the principal components by assuming that after 25ns the fluorescence of that component is negligable as observed in **Figure S3**. By doing this we might miss a possible long contribution in the decay of the intermediate species. This would result in an over estimation of the Solid contribution to the images in our analysis.

Video of the reference species.

We can now use the CPi (τ) base to decompose and display the contribution of the reference species in an image. This means to calculate $c_i(X,Y,t)$ so that

$$I(X,Y,\tau,t) = \sum_i c_i(X,Y,t)REF_i(\tau) = \underset{[C]}{\overset{imp}{\frown}}(X,Y,t)\ \ _{imp}\{[REF](\tau)$$

$$I(X,Y,\tau,t) = \underset{[D]}{\overset{imp}{\frown}}(X,Y,t)\ \ _{4096}\{[CP](\tau)$$

where [C]= [B]$^{-1}$[D]. D_i(X,Y,t) as well as C_i(X,Y,t) are videos. C_i(X,Y,t) are the videos of the concentration of the known species

$$\int_\tau I(X,Y,\tau,t)CPi(\tau)dt = \int_j dj\,(X,Y,t)\int_\tau CPi(\tau)CPi(\tau)dt = \int_j dj\,(X,Y,t)\delta_{ij}$$

$$\int_\tau I(X,Y,\tau,t)CPi(\tau)d\tau = \sum_j d_j\int_\tau CPj(\tau)CPi(\tau)d\tau = d_i$$

The elements d_i(X,Y,t) of the video D can be calculated explicitly since the CP form an orthonormal base.

The integral $\int_\tau I(X,Y,\tau,t)CPi(\tau)dt$ can be easily computed in Pro (v. 6.3) (WaveMetrics Inc., USA) using the weighted histogram command.

These video can be average over time in order to get the images that are displayed in the text (**Figure 4 A,B,C,D,E**). They can be average over space to get the time evolution of the three components during the acquisition. This is displayed on **Figure S4c**.The peaks that are observed on the crystal contribution every 50s can

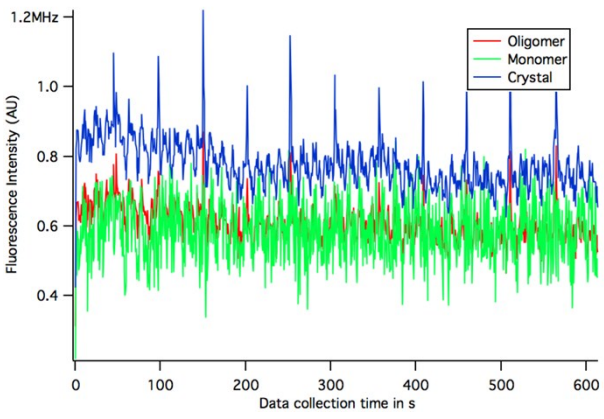

Fig S4d. Intensity of the three components as a function of the collection time that shows the release of long lived particle in the flow.

be interpreted as the regular release of precipitated particle from by the tip of the inner capillary.

The residuals $[R_{FLIM}]=I(X,Y,\tau,t)-[D(X,Y,t)][CP](\tau)$ can be used to identify where data are not well described.

This approach answered the three questions that arise during the analysis of FLIM images : 1) how many fluorescent species are present, 2) what is their decay and 3) where are they located.

The first question is addressed explicitly by PCA. It is addressed on a database of a few decays where many photons have been gathered; thus where the signal over noise ratio is good.

The second question is more difficult to address in the PCA approach. The traditional approach, by fitting with convoluted exponentials, the constraint of the exponentiality and the published values help to define the lifetimes. But in our example, three species are suspected and two reference decays were available. We have construct the third one using one assumption on the order of magnitude of the dominant lifetime.

The third question is simply and robustly answered with the PCA approach. The contribution for any pixel at any time is obtained explicitly as a finite integral. A value is obtained even from very few photons with a noise resistant formula.

S5. Tetra-exponential decay fitting

The fitting curves of the corresponding background-subtracted fluorescence decays were calculated in IGOR Pro (v. 6.3) (WaveMetrics Inc., USA). The fitted curves and their corresponding weighted residuals were shown in **Figure S5**.

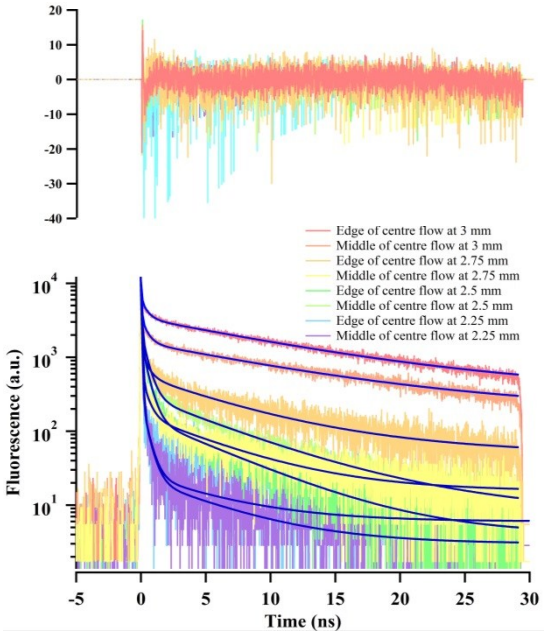

Fig S5. Fluorescence decay curve of the centre flow (background subtracted) from 2.25 mm to 3 mm with fitting curves using tetra-exponential function. Above plot represents the corresponding weighted residuals of the fitting.

References

1 A. Jouyban, *J. Pharm. Pharm. Sci.*, 2008, **11**, 32–58.
2 H. Abdi and L. J. Williams, *Wiley Interdiscip. Rev. Comput. Stat.*, 2010, **2**, 433–459.